






Article

Synthesis, Characterization, Single-Crystal X-ray Structure and Biological Activities of [(Z)-N'-(4-Methoxybenzylidene)benzohydrazide–Nickel(II)] Complex

Inas Al-Qadisy ¹, Abdel-Basit Al-Odayni ^{2,*} , Waseem Sharaf Saeed ² , Ali Alrabie ¹, Arwa Al-Adhrei ¹, Lena Ahmed Saleh Al-Faqeeh ³ , Prem Lama ⁴ , Abdulaziz Ali Alghamdi ⁵  and Mazahar Farooqui ^{1,*}

- ¹ Maulana Azad of Arts, Science and Commerce, P.O. Box 27, Aurangabad 431001, India; inas2015228@gmail.com (I.A.-Q.); aalrabiee1@gmail.com (A.A.); arwa2013_ahmed@yahoo.com (A.A.-A.)
- ² Engineer Abdullah Bugshan Research Chair for Dental and Oral Rehabilitation, College of Dentistry, King Saud University, Riyadh 11545, Saudi Arabia; wsaeed@ksu.edu.sa
- ³ Microbiology Department, Dr. Babasaheb Ambedkar Marathwada University, P.O. Box 27, Aurangabad 431004, India; lenaalfaqeeh8@gmail.com
- ⁴ CSIR-Indian Institute of Petroleum, DHOP Division, Haridwar Road, Mokhampur, Dehradun 248005, India; prem.lama@iip.res.in
- ⁵ Chemistry Department, College of Science, King Saud University, P.O. Box 2455, Riyadh 11451, Saudi Arabia; aalghamdia@ksu.edu.sa
- * Correspondence: aalodayni@ksu.edu.sa (A.-B.A.-O.); mazahar_64@rediffmail.com (M.F.)



Citation: Al-Qadisy, I.; Al-Odayni, A.-B.; Saeed, W.S.; Alrabie, A.; Al-Adhrei, A.; Al-Faqeeh, L.A.S.; Lama, P.; Alghamdi, A.A.; Farooqui, M. Synthesis, Characterization, Single-Crystal X-ray Structure and Biological Activities of [(Z)-N'-(4-Methoxybenzylidene)benzohydrazide–Nickel(II)] Complex. *Crystals* **2021**, *11*, 110. <https://doi.org/10.3390/cryst11020110>

Received: 18 December 2020

Accepted: 23 January 2021

Published: 26 January 2021

Publisher's Note: MDPI stays neutral with regard to jurisdictional claims in published maps and institutional affiliations.



Copyright: © 2021 by the authors. Licensee MDPI, Basel, Switzerland. This article is an open access article distributed under the terms and conditions of the Creative Commons Attribution (CC BY) license (<https://creativecommons.org/licenses/by/4.0/>).

Abstract: (Z)-N'-(4-methoxybenzylidene)benzohydrazide (HL) and its Ni(II) complex (Ni(II)-2L) were synthesized using eco-friendly protocols. The single X-ray crystal structure of Ni(II)-2L was solved. Moreover, the structural properties were evaluated using Fourier transform infrared, proton nuclear magnetic resonance, mass, and Ultraviolet/Visible spectroscopy. The diamagnetic and thermal stability were assessed using magnetic susceptibility and thermogravimetric analysis, respectively. The biological activities of both HL and Ni(II)-2L (62.5–1000 µg/mL) against Gram-positive (*Staphylococcus aureus* and *Streptococcus pyogenes*) and Gram-negative (*Escherichia coli* and *Pseudomonas aeruginosa*) bacterial and fungal (*Candida albicans*, *Aspergillus niger*, and *Aspergillus clavatus*) species were studied using the minimum inhibitory concentration (MIC) tests method in reference to Gentamycin and Nystatin standard drugs, respectively. The results revealed an affordable, environmentally friendly, and efficient synthetic method of HL using water as a green solvent. The Ni(II)-2L complex crystallized in a distorted square planar, $P2_1/n$ space group, and one Ni(II) to two bidentate negatively charged ligand ratio. The analysis of biological activity revealed higher activity of the complex against *S. aureus* and *S. pyogenes* (bacteria) and *A. niger* and *A. clavatus* (fungi) compared to the ligand. However, the highest activity was at a MIC of 62.5 µg/mL for the complex against *S. pyogenes* and for the ligand against *E. coli*. Therefore, both HL and Ni(II)-2L could be promising potential antimicrobials and their selective activity could be an additional benefit of these bioactive materials.

Keywords: hydrazones; nickel complex; crystal structure; biological activity; spectral analysis; green synthesis

1. Introduction

The synthesis of hydrazones and their metal complexes has attracted considerable scientific interest [1]. They are an essential class of biologically active compounds with unique properties, and they exhibit a broad spectrum of physiological and pharmacological activities [2]. However, biological activity is a structure-dependent property. Therefore, various derivatives have been synthesized and adequately investigated. Hydrazones possess an azomethine–NHN = CH– group, formed by the reaction of aldehydes or ketones

with hydrazine or hydrazide motifs. They are a special class of Schiff bases, which are known to exhibit a wide range of interesting biological activities, including antioxidant, antimicrobial, anti-inflammatory, and anticonvulsant properties [3–7]. Moreover, the C=O group in the aroylhydrazones (-C=N-NH-CO-) compounds provides the molecule with an additional donor site, making them a more versatile and effective chelating agent with the ability to form a variety of complexes with different transition ions [5,8,9]. Complexation of aroylhydrazones with metal ions results in more reactive materials due to the presence of both imine and carbonyl groups, and it is an emerging class of Schiff base complexes, reported to have useful antimicrobial [10–12], antioxidant [13], antitumor [14,15], antidepressant [16], analgesic, anti-inflammatory [17], antitubercular [18,19], anti-convulsant [20], and sensor [21] properties.

N'-(4-methoxybenzylidene)benzohydrazide (MBBH) is a type of aroylhydrazones that possesses both hydrazone and carbonyl groups, which may synergistically contribute to their biological activities [22]. Due to their appealing properties, MBBH has been subjected to extensive studies by various researchers [7,13,22–28]. The crystal structure reported in the literature [27] for MBBH indicates that an (*E*)-MBBH structure is the preferred configuration. The methods used for MBBH synthesis are varied and use different solvents and reaction conditions. For instance, Periakaruppan et al. [7] used two methods, employing an optimized ratio of chloroacetic acid and malononitrile in water. However, regardless of the synthetic method, its physicochemical and biological activities were adequately investigated. Despite the straightforward methods available for the synthesis of MBBH, green protocols are always needed. Thus, trying to use readily available and eco-friendly media, such as water, is one target for the future of green chemistry [29], for both small- and large-scale productions.

Nickel (Ni) is a ferromagnetic transition metal with an electron configuration of [Ar] $3d^8 4s^2$. Its most common oxidation state is Ni^{2+} , however, compounds with other oxidation states [30] as well as various geometries including tetrahedral and square planar (4-coordinate), trigonal bipyramidal and square pyramidal (5-coordinate), octahedral (6-coordinate), etc., were also known. Besides its implication in a wide variety of metallurgical processes, it plays a well-defined role in biological systems as well [31]. Since nickel amount in individuals is trace, its deficiency is rare [32]. Yet, nickel is known to be essential, at least, for nine classes of enzymes to be active [31], which involved in some catalytic redox and nonredox chemistries.

The coordination chemistry of hydrazide derivatives such as aroylhydrazones with transition metals has interested many authors [22,33–39]. Nickel(II)-MBBH complex was synthesized by El-Sayed et al. [22]. According to the authors, and depending on the magnetic and spectral analysis, aroylhydrazones can react as a neutral ligand, resulting in octahedral complexes. However, the treatment of such complexes with alkalis leads to their transformation into square planar neutral compounds. Balachandran and George [37] studied the oxidation of some aroylhydrazones, including MBBH, with nickel peroxides and reporting a possible production of 23–41% yields as nickel complexes. However, to the best of our knowledge, no research has been conducted on the crystal structure and biological activities of nickel–MBBH complexes.

Nevertheless, nickel complexes of very close Schiff bases were reported. A square planar structural geometry of nickel-bidentates and an octahedral of nickel-tridentate ones [40–45] were common. In addition, the electron density of the amide oxygen and imine nitrogen of aroylhydrazones, involved in coordination with nickel ions, can be controlled by protonation–deprotonation of the amide nitrogen. Thus, structural geometry could be converted from square planar to octahedral within protonation [22,42], making them potentials in various applications including, chemosensors and photo-conductors as well as pharmaceutical drugs for the treatment of, e.g., cancer, schizophrenia, leprosy, etc. [42].

Therefore, the aim of this work was to synthesize MBBH Schiff base (ligand, HL) and its nickel complex (Ni(II)-2L) using optimized, affordable, and eco-friendly methods. Subsequently, Ni(II)-2L was successfully crystallized, and its crystal structure was determined.

The structural properties were characterized using various spectral, magnetic, and thermal techniques. Additionally, their biological activities against different types of bacterial and fungal species were compared.

2. Materials and Methods

2.1. Chemicals

p-Anisaldehyde (4-Methoxybenzaldehyde) (pAAD; 99%) was purchased from HPLC Lab Reagent (High Purity Laboratory Chemicals Pvt. Ltd, Sarigam INA, India). *N,N*-dimethylformamide (DMF, 99.5%), benzoic hydrazide (BHD, 99%), and polyethylene glycol 400 (PEG, $M_n \approx 400$ g/mol) were obtained from Spectrochem Pvt. Ltd (Mumbai, India). Absolute ethanol (EtOH, 99.9%), dichloromethane (DCM, 99%), ethyl acetate (EA, 99%), nickel(II) nitrate hexahydrate ($\text{Ni}(\text{NO}_3)_2 \cdot 6\text{H}_2\text{O}$, 98%), and ammonium hydroxide (NH_4OH) were obtained from SD Fine Chem Limited (Mumbai, India). Double distilled water was used when needed.

2.2. Microorganisms

Microbes were procured from the “Institute of Microbial Technology” (IMTECH), Chandigarh, India, and used for antimicrobial activity studies: the Gram-positive bacteria *Staphylococcus aureus* (*S. aureus* (MTCC 96)) and *Streptococcus pyogenes* (*S. pyogenes* (MTCC 442)), the Gram-negative bacteria *Escherichia coli* (*E. coli* (MTCC 443)) and *Pseudomonas aeruginosa* (*P. aeruginosa* (MTCC 1688)), and the fungi *Candida albicans* (*C. albicans* (MTCC 227)), *Aspergillus niger* (*A. niger* (MTCC 282)), and *Aspergillus clavatus* (*A. clavatus* (MTCC 1323)) were used in the study.

2.3. Synthesis of (Z)-N'-(4-Methoxybenzylidene) Benzohydrazide Ligand

For comparison, four different reaction pathways (methods i-iv) were used to synthesize the targeted MBBH Schiff base (from here on, this ligand will be referred to as HL) as shown in Figure 1. The reaction progression was monitored using thin-layer chromatography (TLC), where DCM/EA (2:8 volume ratio) is the mobile phase, and silica gel is the stationary phase. After reaction completion, the reaction mixture was poured into ice-cold water and the precipitated title compound was filtered, dried, and kept until use. However, as detailed below, method (i) is conventional, whereas methods (ii-iv) are new and considerably eco-friendly.

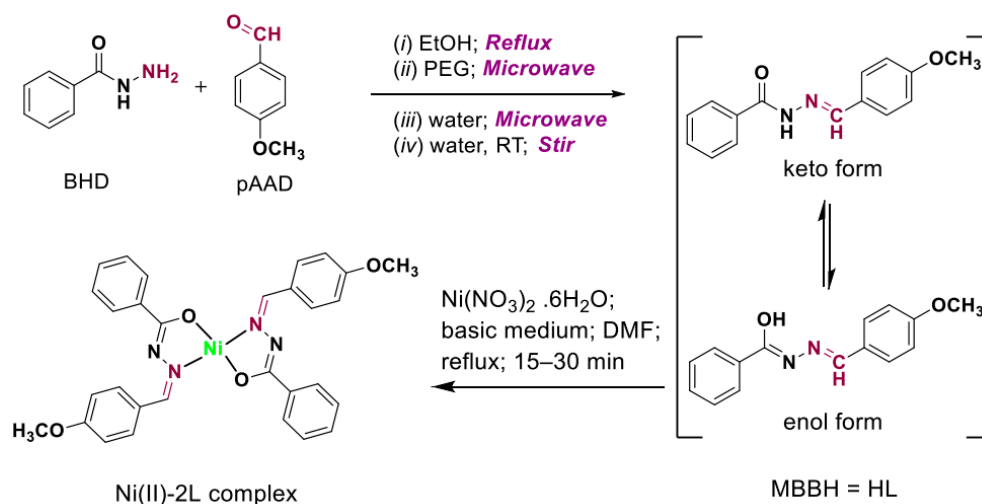


Figure 1. Schematic presentation of the methods used for the synthesis of anisole Schiff base (HL) and its nickel(II) complex (Ni(II)-2L).

Method (i), reflux method. An equimolar of pAAD and BHD (10 mmol each) was refluxed at 70–80 °C for 2 h in 20 mL absolute ethanol.

Method (ii) and (iii), microwave methods. The reactants pAAD and BHD (10 mmol each) were dissolved in 10 mL of either PEG (method (ii)) or water (method (iii)). Then, they were applied into the microwave reactor for 2 min or 20 s, respectively.

Method (iv), stir method. An aqueous solution of the reactants similar to that used in method (iii) was prepared, but the mixture was stirred at room temperature for 30 s to produce the intended Schiff base (HL).

2.4. Synthesis of (Z)-N'-(4-Methoxybenzylidene) Benzo Hydrazide Ni(II) Complex–(Ni(II)-2L)

A nickel(II) complex of HL (denoted Ni(II)-2L) was synthesized using nickel nitrate salt (Figure 1). In a round-bottom flask, 2 mmol (0.508 g) of HL was dissolved in DMF (15 mL), and a nickel salt (1 mmol, 0.291 g) was added in 5 mL of water. The medium was alkalized with the addition of a few drops of NH_4OH . Then, it was heated at ~80 °C under reflux conditions for 30 min. The TLC monitoring test indicated an almost complete reaction in the first 15 min. However, the reaction was continued for 30 min to achieve completeness. Then, it was cooled and left to rest overnight at room temperature. The obtained crystals were filtered, washed with DMF, and dried in vacuo to finally produce orange crystals with an 87% yield. It is worth mentioning that trial synthesis of Ni(II)-2L using EtOH and PEG as reaction mediums was also performed under a similar condition. However, only powder-like microcrystals were observed. Moreover, the microwave-assisted synthesis method using DMF, EtOH, and PEG as reaction mediums (using Ni(II)/ligand mole ratio as 1: 2; the medial was also alkalized using drops of ammonium hydroxide as above) operated for 1.5 min to produce high yields of about 98%. However, only microcrystals were obtained. Thus, only crystals obtained from the reflux method in DMF were used for further studies, including single X-ray analyses.

2.5. Instrumentation

Fourier transform infrared (FTIR) spectra were recorded using a Nicolet iS10 spectrophotometer (Thermo Scientific, Waltham, MA, USA) with a method of attenuated total reflection (ATR; diamond crystal), over a 4000–650 cm^{-1} region with a spectral resolution of 4 cm^{-1} and 16 scans per spectrum. Elemental analysis was performed using a Euro EA3000 CHNS-O analyzer (EuroVector S.p.A. (EVISA), Milan, Italy). Proton and carbon-13 nuclear magnetic resonance (^1H -, ^{13}C -NMR) spectra were obtained at room temperature using a JEOL ECP400 NMR spectroscope (JEOL Ltd., Akishima, Tokyo, Japan). The mass spectra were recorded using an LC-plus Accu-TOF JMS-T100 LP spectrometer (JEOL Ltd., Akishima, Tokyo, Japan) equipped with a DART ion source (IonSense, Saugus, MA, USA) and operated in the +ve-ion mode. Selected peaks were assigned using Mass Centre software (version 1.3.m). Thermogravimetric analysis/differential thermal analysis (TGA/DTA) curves were obtained using a Shimadzu DTG-60H (Kyoto, Japan) thermal analyzer in a platinum cell and operated with a heating rate of 20 °C/min from 25 to 1000 °C and a nitrogen flow of 50 mL/min. Melting points were measured using a CL-726 digital apparatus (IndiaMART Member Since, India). Electronic spectra were recorded over the range of 200–800 nm at room temperature using a UV-1700 spectrophotometer (Shimadzu, Kyoto, Japan) in a DMSO/water (2:8 *v/v*) mix solvent. Molar absorptivity (ϵ , $\text{M}^{-1} \text{cm}^{-1}$) of both HL and Ni(II)-2L (0.0003 M) was analyzed according to Beer-Lambert law at room temperature. Magnetic susceptibility measurements were carried out on solid complex at room temperature (297 K) using a Sherwood Scientific magnetic susceptibility balance (MSB) Mark I (Cambridge, UK), calibrated with a sealed standard manganese(II) chloride solution. The magnetic moment was calculated using Equation (1).

$$\mu_{eff} = 2.48 \sqrt{x_m T} \quad (1)$$

where μ_{eff} is the effective magnetic moment, x_m is the molar susceptibility, and T (K) is the absolute temperature.

2.6. X-ray Crystallography

Diffraction data of the single-crystal structure were collected at 173 K on a Bruker APEX-III photon detector diffractometer equipped with an Oxford Cryosystems, Cryostream 700Plus cryostat. A multilayer monochromator with MoK α radiation ($\lambda = 0.71073 \text{ \AA}$) from an Incoatec I μ S microsource was used. Data reduction was conducted following standard procedures using the Bruker software package SAINT [46], and absorption and other systematic error corrections were performed using SADABS [47,48]. The structures were solved by direct methods using SHELXS-97 and refined using SHELXL-97 [49]. X-Seed [50] was used as the graphical interface for the SHELX program suite. Hydrogen atoms were placed in calculated positions using riding models. The crystallographic data for the Ni(II)-2L complex are provided in Table 1.

Table 1. Crystal structure and refinement details for Ni(II)-2L.

Empirical Formula	C ₃₀ H ₂₆ NiN ₄ O ₄
Formula weight	565.26
Temperature/K	100(2)
Crystal system	monoclinic
Space group	<i>P</i> 2 ₁ / <i>n</i>
<i>a</i> / \AA	11.6165(9)
<i>b</i> / \AA	6.4540(5)
<i>c</i> / \AA	17.9785(14)
α / $^\circ$	90
β / $^\circ$	106.395(3)
γ / $^\circ$	90
Volume/ \AA^3	1293.09(17)
<i>Z</i>	2
Density (calculated)/(g/cm ³)	1.452
μ /mm ⁻¹	0.795
F(000)	588.0
Crystal size/mm ³	0.210 \times 0.200 \times 0.180
Radiation	MoK α ($\lambda = 0.71073$)
2 Θ range for data collection/ $^\circ$	6.74 to 49.998
Index ranges	$-13 \leq h \leq 13, -7 \leq k \leq 7, -21 \leq l \leq 21$
Reflections collected	15,298
Independent reflections	2283 [<i>R</i> _{int} = 0.0353, <i>R</i> _{sigma} = 0.0221]
Data/restraints/parameters	2283/0/179
Goodness-of-fit on <i>F</i> ²	1.054
Final <i>R</i> indexes [<i>I</i> \geq 2 σ (<i>I</i>)]	<i>R</i> ₁ = 0.0245, <i>wR</i> ₂ = 0.0568
Final <i>R</i> indexes [all data]	<i>R</i> ₁ = 0.0290, <i>wR</i> ₂ = 0.0605
Largest diff. peak/hole/e \AA^{-3}	0.27/−0.25

2.7. Biological Studies

A minimum inhibitory concentration (MIC) test was performed using the macro-double dilution method [51]. Generally, material solutions of 62.5–1000 $\mu\text{g/mL}$ were prepared in DMSO in labeled test tubes. A measure of 1 mL of nutrient broth or Sabouraud dextrose and 10 μL of bacteria or fungi strains, respectively, were added to each tube. Then, the tubes were incubated at 37 $^\circ\text{C}$ for 18–24 h, and after that, they were observed for turbidity or growth. Gentamycin of 0.5–1.0 $\mu\text{g/mL}$ and Nystatin of 100 $\mu\text{g/mL}$ were used as standard antibacterial and antifungal drugs, respectively.

3. Results and Discussion

3.1. Synthesis Protocols

The HL was successfully synthesized from anisole and benzoic hydrazide substrates (Figure 1). The conditions of the applied methods and physical properties of the obtained products can be seen in Table 2. It is evident that, regardless of the method of synthesis, the yields of the ligand were highest when the medium was water, with the reaction being

completed within a few seconds. This suggests that methods (iii) and (iv) provide convenient, sufficient, and eco-friendly strategies for the synthesis of HL. However, methods (i) and (ii) resulted in lower yields and required longer reaction durations of up to 2 h. In all cases, ranges of melting points were recorded. However, methods (iii) and (iv) showed a similar melting point of about $156\text{ }^{\circ}\text{C} \pm 2\text{ }^{\circ}\text{C}$. The light-brown color of the product of method (ii) could be due to the solvent effect. Moreover, TLC analysis indicated pure products. However, the products from method (iv) were considered more satisfactory for the subsequent experiments with the advantage of being high yielding at room temperature, in a few seconds, with no heating or catalyst required, and using water as a green medium.

Table 2. Physical properties of the synthesized N' -(4-methoxybenzylidene)benzohydrazide Schiff (HL) base and its nickel(II) complex (Ni(II)-2L).

Comp.	Synthesis Strategy				Physical Properties		
	Methods	Type	Medium	Reaction Time	Color	Melting Point	Yield (%)
HL	Method (i)	Reflux	EtOH	2 hrs	White	153 ± 3	98
	Method (ii)	Microwave	PEG	2 min	Light-brown	152 ± 2	79
	Method (iii)	Microwave	Water	20 sec	White	156 ± 2	99
	Method (iv)	Stir	Water	30 sec	White	156 ± 2 ; (DTA, 160)	99
Ni(II)-2L complex	Reflux		DMF	15 min	Orange crystal	>300; (DTA, 298)	87
	Microwave-assisted synthesis		DMF	90 sec	Orange microcrystals	>300	98

Crystals of the Ni(II)-2L complex of sufficient sizes ($0.21 \times 0.20 \times 0.18\text{ mm}$) for single X-ray analysis were acquired in DMF at $80\text{ }^{\circ}\text{C}$. Noticeably, the fast production of Ni(II)-2L under microwave conditions only resulted in a powder-like precipitate making it less favorable for further experiments conducted herein.

3.2. Analytical Characterization

3.2.1. Spectral Analysis

Observed and estimated weight percentages of the elements C, H, N, and O in both HL and Ni(II)-2L are shown in Table 3. The consistency between the observed and calculated percentage of atoms indicates the successful synthesis of the target compounds, which is further supported by a single X-ray and other analytical methods.

Table 3. Analytical data of the N' -(4-methoxybenzylidene)benzohydrazide (HL) ligand and its nickel(II) complex (Ni(II)-2L).

Compound	Chemical Formula	MW	Elemental Analysis (wt %); Found (Calculated)			
			C	H	N	O
HL	$\text{C}_{15}\text{H}_{14}\text{N}_2\text{O}_2$	254.29	70.93 (70.85)	5.62 (5.55)	11.10 (11.02)	12.60 (12.58)
Ni(II)-2L	$\text{C}_{30}\text{H}_{26}\text{N}_4\text{NiO}_4$	565.26	64.05 (63.75)	4.75 (4.64)	9.94 (9.91)	11.35 (11.32)

Figure 2 shows the FTIR spectra of HL and Ni(II)-2L. In the spectrum of HL, the medium intensity broadband at 3414 cm^{-1} possibly represents the OH of the iminol form while the weak band at 3181 cm^{-1} represents NH (amide-iminol tautomerism), which diminished in the Ni(II)-2L spectrum due to coordination [25,52]. The $\nu(\text{C}=\text{O})$ band in the HL spectra was clear at 1639 cm^{-1} which disappeared after complexation, indicating enol form. Moreover, the observed shift in the band of $\nu(\text{C}=\text{N})$ toward lower energies (from 1601 to 1591 cm^{-1}) confirms their contribution in complexation with nickel [22]. The absorption bands of C-H, C=C, C-C, C-N, and C-O are assigned in the spectrum. As metal-organic bonds are usually weak and found in the fingerprint mid-IR region, following them is difficult due to their overlap with skeletal, ring deformation, and bending modes. However, compared with the parent spectra of HL, a new band was observed at 583 cm^{-1} , which

could be speculated as a Ni-O bond in Ni(II)-2L. Additionally, the band found at 461 cm^{-1} in Ni(II)-2L was for Ni-N [53].

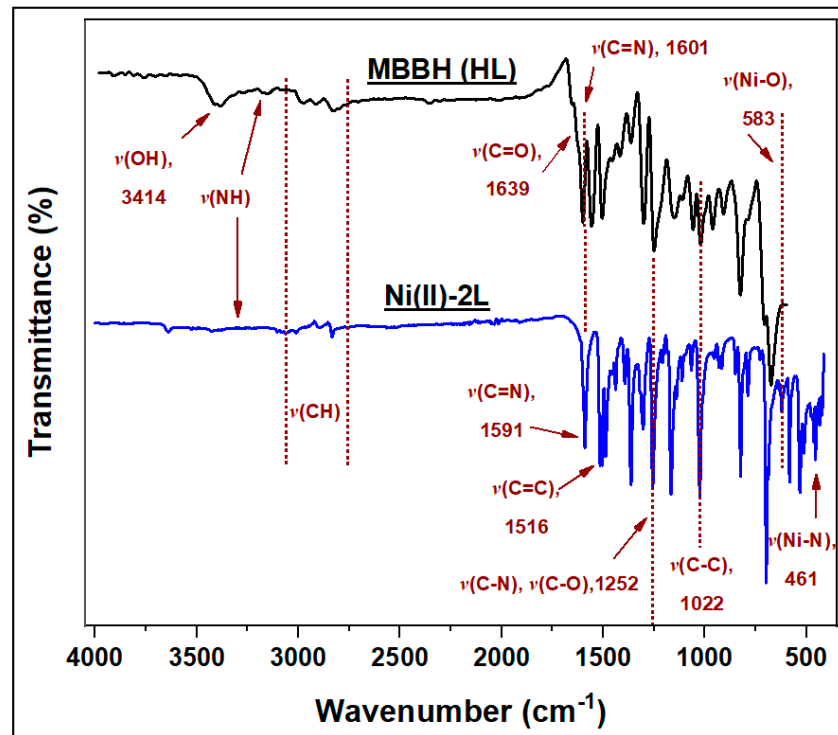


Figure 2. Fourier transform infrared spectra of the N' -(4-methoxybenzylidene)benzohydrazide (HL) ligand and its nickel(II) complex (Ni(II)-2L).

The structure of the ligand was strictly confirmed using ^1H NMR analysis, as shown in Figure 3. The type of H-groups in the molecule was assigned in the spectrum. Furthermore, peak integrations indicated the number of protons in each group. These results are in agreement with those previously reported in the literature [25,54].

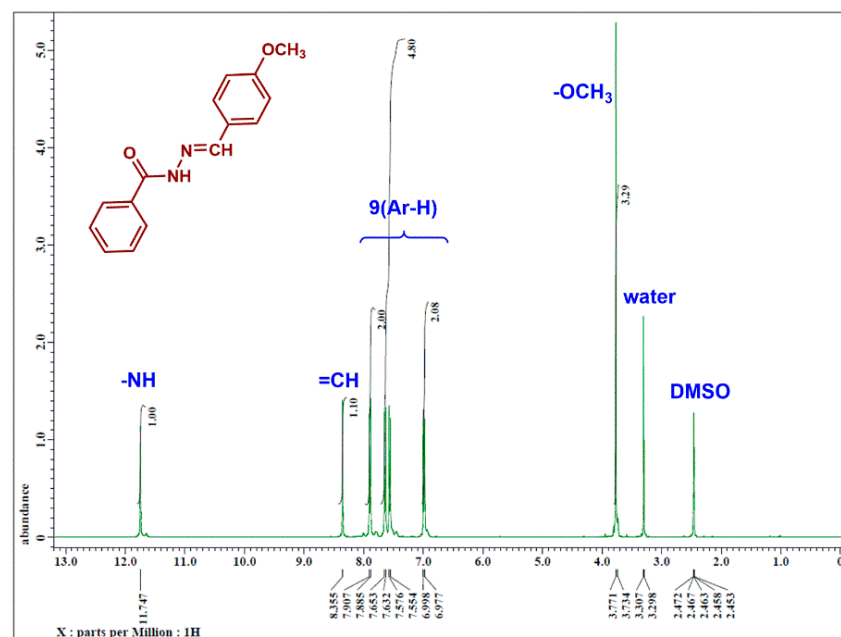


Figure 3. ^1H NMR spectrum of N' -(4-methoxybenzylidene) benzohydrazide (HL) in CDCl_3 .

The mass spectra (obtained in a positive ionization mode, ESI+) and fragmentation pathway of the HL ligand are illustrated in Figure 4. The protonated molecular ion $[M+H]^+$ with an m/z of 255.1137 was the most intense fragment (the base peak), possibly due to the resonance stabilization of the positive charge over the molecule. Fragments with m/z values of 277.0977, 531.2043, and 785.2965 were assigned to the sodium adducts, $[M+Na]^+$, $[2M+Na]^+$, and $[3M+Na]^+$, respectively [55–57]. All these results provide evidence of the chemical structure of HL and, thus, its successful synthesis.

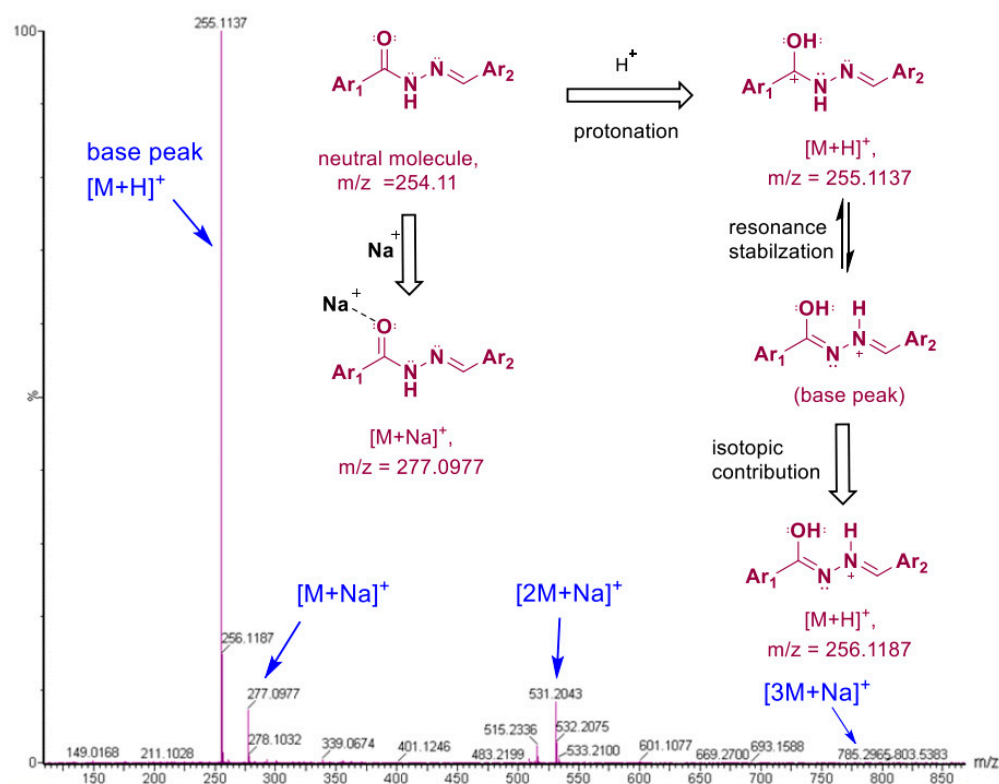


Figure 4. Mass spectrum (ES+ mode) of $N'-(4\text{-methoxybenzylidene})\text{benzohydrazide}$ (HL) Schiff base and its suggested fragmentation pathways.

The electronic spectra of both HL and (Ni(II)-2L) are shown in Figure 5 and Table 4. The spectrum of the ligand revealed a low intense peak at 243 nm and high intense overlapped peaks with maxima at 315 nm and shoulder at ca 296 nm for $L-L^*$ transitions ($\pi-\pi^*$ and $n-\pi^*$). The spectrum of the complex shows a more or less similar pattern to that of the ligand in the region below 350 nm. However, additional weak bands at lower energies (above 350 nm) possibly responsible for its orange color, were observed. The two bands at 372 and 411 nm could be assigned to the ligand to metal charge transfer (LMCT) transition. The other two bands at 433 and 574 nm were assigned to spin allowed $d-d$ transitions, $^1A_{1g} \rightarrow ^1A_{2g}$ and $^1A_{1g} \rightarrow ^1B_{1g}$, respectively, which characterize the square planar geometry around Ni(II) ion [58–60].

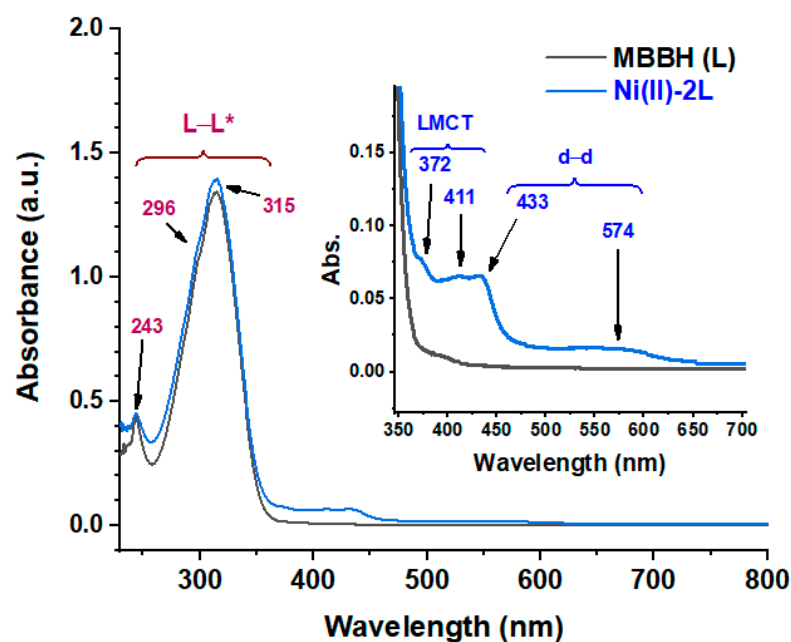


Figure 5. Electronic spectra of the *N'*-(4-methoxybenzylidene)benzohydrazide (HL) ligand and its nickel(II) complex (Ni(II)-2L). The inset is a magnification view in the range of 350–700 nm.

Table 4. Electronic transitions and magnetic moment data of *N'*-(4-methoxybenzylidene)benzohydrazide (HL) ligand and its nickel(II) complex (Ni(II)-2L).

Compound	Abs (a.u.)	λ (nm)	ϵ (M ⁻¹ cm ⁻¹)	Assignment	μ_{eff} (BM)	Geometry
HL	0.445	243	148	π - π^*	-	-
	1.022	296	341	π - π^*		
	1.344	315	448	n- π^*		
Ni(II)-2L	0.445	243	148	π - π^*	0	Square planar
	1.085	296	362	π - π^*		
	1.394	315	465	n- π^*		
	0.081	372	27	LMCT		
	0.066	411	22	LMCT		
	0.066	433	22	$^1A_{1g} \rightarrow ^1A_{2g}$		
	0.017	574	6	$^1A_{1g} \rightarrow ^1B_{1g}$		

3.2.2. Magnetic Moment

The magnetic moment measurement of Ni(II)-2L revealed diamagnetic character with an effective magnetic moment of zero ($\mu_{eff} = 0$, BM), Table 4. This means that all electrons were paired, indicating square planar coordination, confirming a strong ligand coordinated on its enol form and resulting in a neutral complex. This result is consistent with literature [22,61] and is supported by X-ray crystal structure.

3.2.3. Thermal Analysis

The thermogravimetric analysis of both the HL Schiff base and its nickel(II) complex (Ni(II)-2L) was also performed, under nitrogen atmosphere, for stability assessment. The obtained TGA/DTA thermograms and fragmentation patterns are shown in Figures 6 and 7, respectively, while the data are presented in Table 5. In the thermograms of HL, 9.5% of moisture was lost first at a derivative TGA (DrTGA) of 83 °C, with endothermic peaks at 89 °C. An endothermic peak at DTA of 160 °C with no TGA mass loss was assigned to the HL melting point. However, one step endothermic (DTA 337°C) decomposition

of HL is observed at 341 °C (DrTGA) with a mass loss of 90.5% (no mass residue can be detected). Additional endothermic peaks, e.g., at 387 °C and 433 °C, were also detected but not assignable. However, it might be a type of allotropic transformation of carbonaceous materials before final decomposition. The thermal stability of the Ni(II)-2L complex was similar to that of the ligand, meaning that the main decomposition was centered at 341 °C with a mass loss of 42.3%. However, three stages of decomposition were identified. The first stage, below 296 °C, was accompanied by a mass loss of 4.6%, which was estimated as 5.3%, due to the loss of two methyl groups (2(-CH₃)). The second stage occurred between 297 °C and 379 °C (with a DrTGA max at 342 °C), with a weight loss of 42.3% due to the elimination of 2[-C₇H₅NO] fragments, losing the major part of the complex through an endothermic process with DTA max at 340 °C. The third step in the TGA curve indicated a stepwise decomposition above 380 °C, centered at 462 °C, with a mass loss of 30.4% ascribed to the removal of C₈H₄N₂O, leaving a residual mass of 22.8%, which was estimated as 24.1%, assigned to metal carbons (NiC₆H₆) [62].

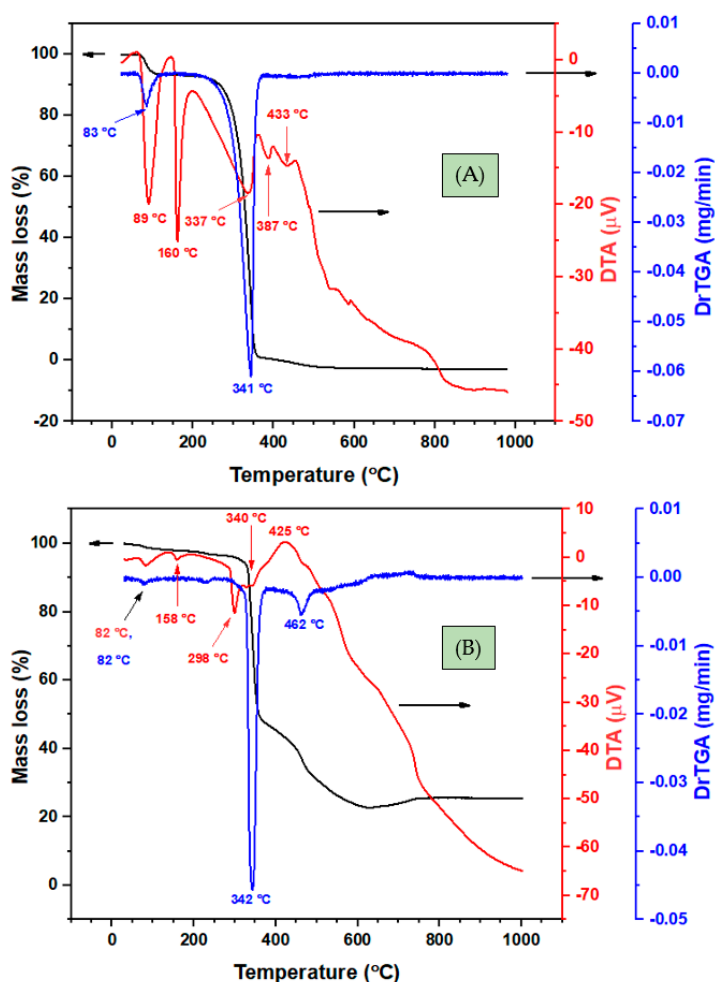


Figure 6. Thermogravimetric analysis (TGA) (black), derivative (Dr)-TGA (blue), and differential thermal analysis (DTA) (red) curves of (A) the *N'*-(4-methoxybenzylidene)benzohydrazide (HL) ligand and (B) its nickel complex (Ni(II)-2L).

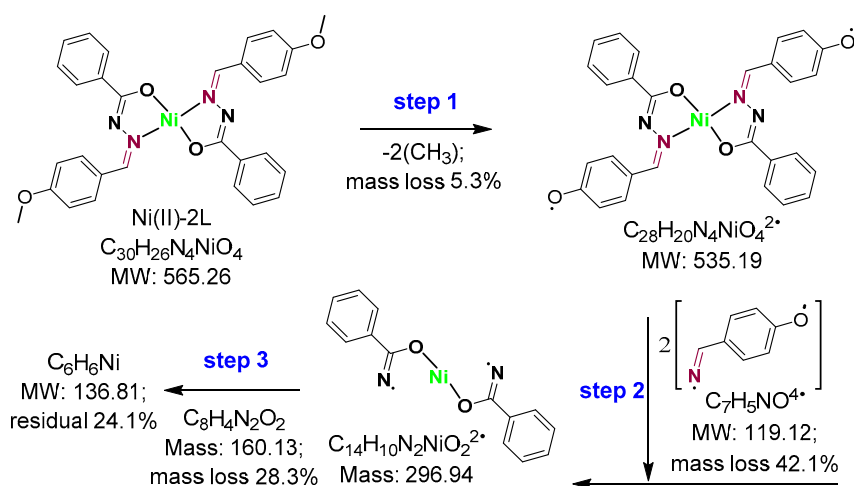


Figure 7. Schematic presentation of suggested thermogravimetric analysis fragmentation pattern, including the predicted mass-loss percentage.

Table 5. Thermogravimetric analysis (TGA), derivative (Dr)-TGA, and differential thermal analysis (DTA) data of the *N'*-(4-methoxybenzylidene)benzohydrazide (HL) Schiff base and Ni(II)-2L.

Comp.	Step	Temp. (°C)	DrTGA max (°C)	DTA Max (°C)		Mass Loss (%)		Evolved Moieties	Residue (%)
				Endo	Exo	Obs.	Calc.		
HL	1	66–108	83	89	-	9.5	9.6	1.5 H ₂ O, moisture	-
	2	250–380	341	337, 387, 433	-	90.5	90.4	100% ligand	-
Ni(II)-2L	1	55–296	82, 158	82, 225	-	4.6	5.3	2(-CH ₃)	NiC ₆ H ₆ ; Obs. 22.8, Calc. 24.1
	2	297–379	342	340, 372	-	42.3	42.1	2[C ₇ H ₅ NO]	
	3	380–627	462	425	multi	30.4	28.3	C ₈ H ₄ N ₂ O ₂	

Comp., compound; Temp., temperature range; Endo, endothermic; Exo, exothermic process.

3.3. Crystal Structure

According to the obtained single-crystal structure data, nickel complex crystallized as a discrete unit in the $P2_1/n$ space group. The negatively charged ligand bound to Ni(II) ions through the oxygen atom (O1) and the secondary aldimine nitrogen atom (N2). One full Ni(II) ion was bound to two negatively charged ligands in the distorted square planer (hybridization- dsp^2) geometry (Figure 8). The overall view along the ac -plane formed by the discrete nickel complex is shown in Figure 9. As the complex is discrete in nature, it is stabilized by the weak van der Waals interactions between the discrete units. No such hydrogen bonding interactions were found in the overall structure. The four donor atoms were provided by the two bidentate chelates ligand, HL. The complex was planar within Ni-O1 (and Ni-O1') of 1.8403(11) and Ni-N (and Ni-N') of 1.8703(13) Å bonds length, and O1-Ni-N2 (and O1'-Ni-N2') of 83.70(5) and O1-Ni-N2' (and O1'-Ni-N2) bond angles around metal. Selected bond lengths and angles are provided in Table 6. However, the complete list of molecular geometry, including bond lengths (Table S1) and bond angles (Table S2) and the crystallographic information files (cif) are available in the supplementary files. The structure reported by Joseph et al. [40] forms 1:1 metal complex with the ligand whereas in our Ni(II)-2L structure the metal to ligand ratio is 1:2. Even though both complexes are based on carbohydrazide derivatives, our Ni(II)-2L structure is without any lattice solvent molecule and the nickel center is in distorted square planer geometry whereas the reported structure has Ni (II) ion in distorted octahedral geometry with lattice *N,N'*-dimethylformamide molecules. Aroylhydrazones-based square-planar Ni(II) complexes reported by Mondal et al. [42] are somewhat similar to our Ni(II)-2L structure. The reported Ni-O bond distances in the two square-planar complexes are 1.8366 (15) and 1.8283(11), whereas the Ni-N bond distances are 1.8840(16) and 1.8912(14), respectively. These bond

distances are almost similar with slight variation as compared to our Ni(II)-2L structure. The presence of NH₂ group of anthraniloyl moieties in one of the complexes reported by Mondal and co-workers leads to an intramolecular hydrogen bonding. However, no such intramolecular or intermolecular hydrogen bonding was seen in our Ni(II)-2L case. In addition, there are few other similar such structures are reported in the literature [43–45].

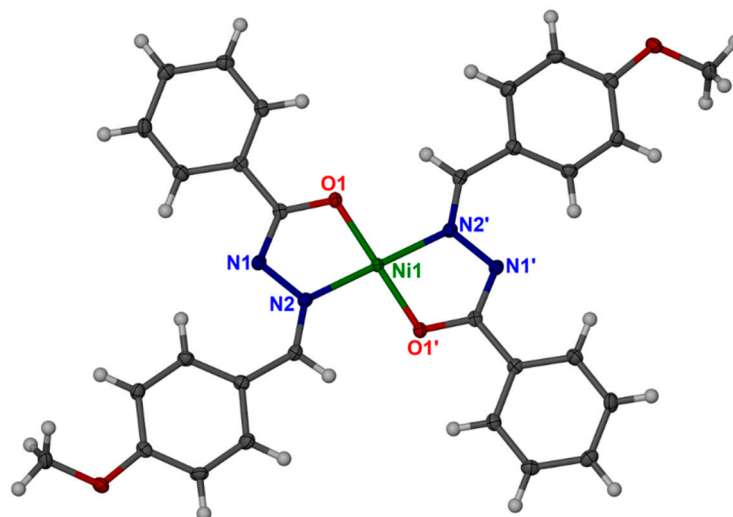


Figure 8. Coordination mode of Ni(II) ion in the Ni(II)-2L with 50% probability thermal ellipsoid (O1', N1' and N2' are symmetry generated atoms; the symmetry transformation implied for each additional symmetry label atoms: 1-x, -y, 1-z).

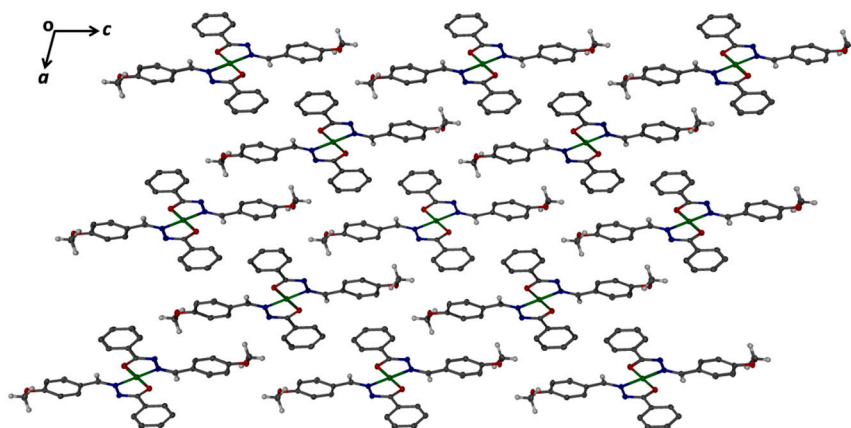


Figure 9. View showing the arrangement of discrete units of the Ni(II)-2L along *ac*-plane. Aromatic hydrogen atoms are removed for clarity.

Table 6. Selected bond length (Å) and bond angles (°) for Ni(II)-2L.

Bond Lengths			Bond Angles			
Atom	Atom	Length (Å)	Atom	Atom	Atom	Angle (°)
Ni1	O1	1.8403(11)	O1	Ni1	O1 ¹	180.0
Ni1	O1 ¹	1.8403(11)	O1	Ni1	N2	83.70(5)
Ni1	N2	1.8703(13)	O1 ¹	Ni1	N2	96.30(5)
Ni1	N2 ¹	1.8703(13)	O1	Ni1	N2 ¹	96.30(5)
O1	C7	1.3016(19)	O1 ¹	Ni1	N2 ¹	83.70(5)
N1	N2	1.3976(19)	N2	Ni1	N2 ¹	180.0

3.4. Biological Activities

The results of the antimicrobial activity tests of both HL and Ni(II)-2L are provided in Table 7. The minimal inhibitory concentration (MIC) values revealed higher activity (lower MIC) of HL against Gram-negative bacteria and lower activity against Gram-positive bacteria. Conversely, the complex activity was higher against Gram-positive bacteria and less active against Gram-negative bacteria. The highest activity (i.e., the lowest MIC) of HL and Ni(II)-2L were against *E. coli* and *S. pyogenes*, respectively, and both had a MIC of 62.5 µg/mL. The MIC tests against fungal strains revealed similar activity of the complex against *A. niger* and *A. clavatus* with MICs of 500 µg/mL, while it seems inactive against *C. albicans*. However, HL was more active against *C. albicans* (MIC of 500 µg/mL) and less active against both *A. niger* and *A. clavatus*. Despite the obtained moderate activity of the tested compounds, their activities were still lower than the standard drugs against all microbes under investigation.

Table 7. Antimicrobial activities of the N'-(4-methoxybenzylidene)benzohydrazide (HL) ligand and its nickel complex (Ni(II)-2L).

Compound	Minimal Inhibition Concentration (MIC) (µg/mL)						
	Bacteria Species				Fungal Species		
	Gram-Positive		Gram-Negative		<i>C. albicans</i>	<i>A. niger</i>	<i>A. clavatus</i>
	<i>S. aureus</i>	<i>S. pyogenes</i>	<i>E. coli</i>	<i>P. aeruginosa</i>			
HL	500	250	62.5	125	500	1000	1000
Ni(II)-2L	125	62.5	125	250	>1000	500	500
Gentamycin	0.25	0.5	0.05	1	-	-	-
Nystatin	-	-	-	-	100	100	100

The biological properties of bioactive compounds can be rationalized on the basis of their structural differences as well as the cell-wall chemistry of microorganisms. The biological activity of organic compounds is associated with many factors. Some of these factors are the stability, concentration, ability to form hydrogen bonds with active centers of the bacteria cell constituents, and ability to inhibit enzyme function [63]. Moreover, the antimicrobial activity of a complex is governed by various factors, including the chelate effect of the ligand, the type of the donor atoms, the charge, and the geometrical structure of the complex [64]. Both HL and the Ni(II)-2L were comparatively active against bacteria and fungi strains. The ligand can be selectively used for *E. coli* inhibition; however, the complex is more effective against *S. pyogenes*. It is worth mentioning that the lipophilicity character of a compound is more favorable in terms of antimicrobial activity. Thus, according to the chelation theory, the ligand activity may be enhanced after coordination [65,66], which explains that a decrease in polarizability of the metal could enhance the lipophilicity of the complexes. This facilitates the compound penetration into the lipid membranes and blocks the metal-binding sites in the enzymes of microorganisms, the action that could disturb the respiration process and protein synthesis, leading to microorganism growth inhibition.

4. Conclusions

An eco-friendly, low-cost, and efficient method for the synthesis of MBBH Schiff base (HL) was established utilizing water as a green solvent. Ni(II)-2L single crystal was synthesized in DMF-based alkaline media with stirring at about 80 °C. Characterization using FTIR, ¹HNMR, UV/Vis, mass, and TGA indicated material integrity and successful synthesis. Crystallography showed the distorted square planar geometry of the complex with an ion to ligand ratio of 1:2, organized within the space group of *P2₁/n* and monoclinic crystal. The ligand was involved in the crystal structure in its enol form, resulting in a neutral complex as confirmed by a single X-ray analysis. The antimicrobial activity studies indicated that both the ligand and its nickel complex (Ni(II)-2L) are effective, with an overall better activity of the complex compared with the ligand. Interestingly, selective

activity of both materials was observed, e.g., Ni(II)-2L was more selective for *S. pyogenes* (G-positive bacteria) with a MIC of 62.5 µg/m, while it seems that it had no effect on *C. albicans* (fungi). Similarly, the highest activity of the ligand was against *E. coli* (62.5 µg/mL) with an overall negligible effect on fungi. Therefore, it might be concluded that HL and Ni(II)-2L are promising antimicrobials with selective properties against targeted species and, thus, deserve further investigation in terms of, e.g., testing other microorganisms and protocols.

Supplementary Materials: The following are available online at <https://www.mdpi.com/2073-4352/11/2/110/s1>, Crystallographic information files (cif) of the title compound (Ni(II)2L), Table S1: Bond length for the Ni(II)-2L complex, Table S2: Bond angles for the Ni(II)-2L complex.

Author Contributions: Conceptualization, I.A.-Q. and M.F.; formal analysis, A.-B.A.-O. and W.S.S.; funding acquisition, A.A.A.; investigation, I.A.-Q., A.A., A.A.-A., L.A.S.A.-F. and P.L.; methodology, I.A.-Q., L.A.S.A.-F. and P.L.; supervision, M.F.; visualization, A.-B.A.-O. and W.S.S.; writing—original draft, I.A.-Q.; writing—review and editing, A.-B.A.-O. and M.F. All authors have read and agreed to the published version of the manuscript.

Funding: The authors extend their appreciation to the Deanship of Scientific Research at King Saud University for funding this work through Research Group No. RGP-1438-040.

Data Availability Statement: All the data supporting the findings of this study are available within the article and supplementary materials.

Acknowledgments: Prem Lama gratefully acknowledges financial support from the Department of Science and Technology (DST), New Delhi in the form of a DST-INSPIRE Faculty award [DST/INSPIRE/04/2017/000249].

Conflicts of Interest: The authors declare no conflict of interest.

References

1. Rajarajan, M.; Senbagam, R.; Vijayakumar, R.; Balaji, S.; Manikandan, V.; Vanangamudi, G.; Thirunarayanan, G. Synthesis, spectral correlations and antimicrobial activities of substituted 4-((E)-2-benzylidenehydrazinyl) benzonitriles. *Indian J. Chem.* **2016**, *55*, 197–206.
2. Chohan, Z.H.; Sherazi, S.K. Biological role of cobalt (II), copper (II) and nickel (II) metal ions on the antibacterial properties of some nicotinoyl-hydrazine derived compounds. *Metal-Based Drugs* **1997**, *4*, 69–74. [[CrossRef](#)] [[PubMed](#)]
3. Belkheiri, N.; Bouguerne, B.; Bedos-Belval, F.; Duran, H.; Bernis, C.; Salvayre, R.; Nègre-Salvayre, A.; Baltas, M. Synthesis and antioxidant activity evaluation of a syringic hydrazones family. *Eur. J. Med. Chem.* **2010**, *45*, 3019–3026. [[CrossRef](#)] [[PubMed](#)]
4. Deeb, A.; El-Mariah, F.; Hosny, M. Pyridazine derivatives and related compounds. Part 13: Synthesis and antimicrobial activity of some pyridazino [3',4':3,4] pyrazolo [5, 1-c]-1,2,4-triazines. *Bioorg. Med. Chem. Lett.* **2004**, *14*, 5013–5017. [[CrossRef](#)]
5. Kajal, A.; Bala, S.; Sharma, N.; Kamboj, S.; Saini, V. Therapeutic potential of hydrazones as anti-inflammatory agents. *Int. J. Med. Chem.* **2014**, *2014*, 1–11. [[CrossRef](#)]
6. Kaushik, D.; Khan, S.A.; Chawla, G.; Kumar, S. N'-[(5-chloro-3-methyl-1-phenyl-1H-pyrazol-4-yl) methylene] 2/4-substituted hydrazides: Synthesis and anticonvulsant activity. *Eur. J. Med. Chem.* **2010**, *45*, 3943–3949. [[CrossRef](#)]
7. Periakaruppan, P.; Abraham, R.; Mahendran, K.; Ramanathan, M. Simple synthesis of hydrazones with quorum quenching activity at room temperature in water. *Environ. Chem. Lett.* **2018**, *16*, 1063–1067. [[CrossRef](#)]
8. Cornelissen, J.P.; Van Diemen, J.H.; Groeneveld, L.R.; Haasnoot, J.G.; Spek, A.L.; Reedijk, J. Synthesis and properties of isostructural transition-metal (copper, nickel, cobalt, and iron) compounds with 7,7',8,8'-tetracyanoquinodimethanide (1-) in an unusual monodentate coordination mode: Crystal structure of bis (3,5-bis (pyridin-2-yl)-4-amino-1,2,4-triazole) bis (7,7',8,8'-tetracyanoquinodimethanido) copper (II). *Inorg. Chem.* **1992**, *31*, 198–202.
9. Rawat, P.; Singh, R. Synthesis and study on aroylhydrazones having cyanovinylpyrrole. *Arab. J. Chem.* **2019**, *12*, 2384–2397. [[CrossRef](#)]
10. Maheswari, R.; Manjula, J. Synthesis, Characterization and Biological Applications of Benzohydrazide derivatives. *Int. J. Appl. Res.* **2015**, *1*, 587–592.
11. Raj, V. Review on the Pharmacological Activities of Hydrazones derivatives. *EC Pharm. Sci.* **2016**, *2*, 278–306.
12. Therese, S.K.; Geethamalika, G. Synthesis, Characterization and Anti Mycobacterial Activity of Novel Hydrazones. *Orient. J. Chem.* **2017**, *33*, 335–345. [[CrossRef](#)]
13. Taha, M.; Ismail, N.H.; Jamil, W.; Yousuf, S.; Jaafar, F.M.; Ali, M.I.; Kashif, S.M.; Hussain, E. Synthesis, evaluation of antioxidant activity and crystal structure of 2, 4-dimethylbenzoylhydrazones. *Molecules* **2013**, *18*, 10912–10929. [[CrossRef](#)] [[PubMed](#)]

14. Wardakhan, W.W.; Sherif, S.M.; Mohareb, R.M.; Abouzied, A.S. The Reaction of Cyanoacetylhydrazine with Furan-2-Aldehyde: Novel Synthesis of Thiophene, Azole, Azine and Coumarin Derivatives and Their Antitumor Evaluation. *Int. J. Org. Chem.* **2012**, *2*, 321–331. [[CrossRef](#)]
15. Tyagi, P.; Chandra, S.; Saraswat, B. Ni (II) and Zn (II) complexes of 2-((thiophen-2-ylmethylene) amino) benzamide: Synthesis, spectroscopic characterization, thermal, DFT and anticancer activities. *Spectrochim. Acta A Mol. Biomol. Spectrosc.* **2015**, *134*, 200–209. [[CrossRef](#)]
16. Mohareb, R.; El-Sharkawy, K.; Hussein, M.; El-Sehrawi, H. Synthesis of hydrazide-hydrazone derivatives and their evaluation of antidepressant, sedative and analgesic agents. *J. Pharm. Sci. Res.* **2010**, *2*, 185–196.
17. Salgın-Gökşen, U.; Gökhan-Kelekçi, N.; Göktaş, Ö.; Köysal, Y.; Kılıç, E.; Işık, Ş.; Aktay, G.; Özalp, M. 1-Acylthiosemicarbazides, 1,2,4-triazole-5 (4H)-thiones, 1,3,4-thiadiazoles and hydrazones containing 5-methyl-2-benzoxazolinones: Synthesis, analgesic-anti-inflammatory and antimicrobial activities. *Bioorg. Med. Chem.* **2007**, *15*, 5738–5751. [[CrossRef](#)]
18. Eldehna, W.M.; Fares, M.; Abdel-Aziz, M.M.; Abdel-Aziz, H.A. Design, synthesis and antitubercular activity of certain nicotinic acid hydrazides. *Molecules* **2015**, *20*, 8800–8815. [[CrossRef](#)]
19. Joshi, S.; More, Y.; Vagdevi, H.; Vaidya, V.; Gadaginamath, G.; Kulkarni, V. Synthesis of new 4-(2,5-dimethylpyrrol-1-yl)/4-pyrrol-1-yl benzoic acid hydrazide analogs and some derived oxadiazole, triazole and pyrrole ring systems: A novel class of potential antibacterial, antifungal and antitubercular agents. *Med. Chem. Res.* **2013**, *22*, 1073–1089. [[CrossRef](#)]
20. Dimmock, J.R.; Vashishtha, S.C.; Stables, J.P. Anticonvulsant properties of various acetylhydrazones, oxamoylhydrazones and semicarbazones derived from aromatic and unsaturated carbonyl compounds. *Eur. J. Med. Chem.* **2000**, *35*, 241–248. [[CrossRef](#)]
21. Pegu, R.; Mandal, R.; Guha, A.K.; Pratihari, S. A selective ratiometric fluoride ion sensor with a (2,4-dinitrophenyl) hydrazine derivative of bis (indolyl) methane and its mode of interaction. *New J. Chem.* **2015**, *39*, 5984–5990. [[CrossRef](#)]
22. El Sayed, L.; Iskander, M. Coordination compounds of hydrazine derivatives with transition metals—III: The reaction of aroyl hydrazones with Ni (II) and Cu (II) salts. *J. Inorg. Nucl. Chem.* **1971**, *33*, 435–443. [[CrossRef](#)]
23. Dimova, V.; Jankulovska, M. QSAR Modeling of Antimicrobial Activity of some p-substituted Aromatic Hydrazones. *J. Scient. Ind. Res.* **2017**, *76*, 550–555.
24. Saleem, H.; Subashchandrabose, S.; Babu, N.R.; Padusha, M.S.A. Vibrational spectroscopy investigation and density functional theory calculations on (E)-N'-(4-methoxybenzylidene) benzohydrazide. *Spectrochim. Acta A Mol. Biomol. Spectrosc.* **2015**, *143*, 230–241. [[CrossRef](#)] [[PubMed](#)]
25. Alam, M.S.; Lee, D.-U. Syntheses, crystal structure, Hirshfeld surfaces, fluorescence properties, and DFT analysis of benzoic acid hydrazone Schiff bases. *Acta A Mol. Biomol. Spectrosc.* **2015**, *145*, 563–574. [[CrossRef](#)] [[PubMed](#)]
26. Jankulovska, M.; Čolančeska-Rađenović, K.; Dimova, V.; Spirevska, I.; Makreski, P. Synthesis and characterization of new p-substituted aromatic hydrazones. *Org. Chem. An Ind. J.* **2012**, *8*, 326–334.
27. Gou, J.-X.; Song, M.-Z.; Fan, C.-G.; Yang, Z.-N. (E)-N'-(4-Methoxybenzylidene) benzohydrazide. *Acta Cryst. E* **2009**, *65*, 3207–3213. [[CrossRef](#)]
28. Tumkevičius, S.; Mekuskiene, G.; Gefenas, V.; Vainilavicius, P. Substituent effect on proton chemical shifts of amide and azomethine groups of arylidenehydrazides of 5-substituted 2-pyrimidine-carboxylic acids and their aromatic analogs. *Chemija* **2005**, *16*, 65–68.
29. Al-Qadisy, I.; Saeed, W.S.; Al-Odayni, A.-B.; Ahmed Saleh Al-Faqeeh, L.; Alghamdi, A.A.; Farooqui, M. Novel metformin-based schiff bases: Synthesis, characterization, and antibacterial evaluation. *Materials* **2020**, *13*, 514. [[CrossRef](#)]
30. Wang, H.; Butorin, S.M.; Young, A.T.; Guo, J. Nickel oxidation states and spin states of bioinorganic complexes from nickel L-edge X-ray absorption and resonant inelastic X-ray scattering. *J. Phys. Chem. C* **2013**, *117*, 24767–24772. [[CrossRef](#)]
31. Maroney, M.J.; Ciurli, S. Bioinorganic Chemistry of Nickel. Multidisciplinary Digital Publishing Institute. *Inorganics* **2019**, *7*, 131. [[CrossRef](#)]
32. Kumar, S.; Trivedi, A. A review on role of nickel in the biological system. *Int. J. Curr. Microbiol. Appl. Sci.* **2016**, *5*, 719–727. [[CrossRef](#)]
33. Iskander, M.; Zayan, S.; Khalifa, M.; El-Sayed, L. Coordination compounds of hydrazine derivatives with transition metals—VI: The reaction of aroylhydrazines with nickel (II), cobalt (II) and copper (II) salts. *J. Inorg. Nucl. Chem.* **1974**, *36*, 551–556. [[CrossRef](#)]
34. Wiegand, R.G. The formation of pyridoxal and pyridoxal 5-phosphate hydrazones. *J. Am. Chem. Soc.* **1956**, *78*, 5307–5309. [[CrossRef](#)]
35. Hrušková, K.; Potůčková, E.; Hergeslova, T.; Liptakova, L.; Hašková, P.; Mingas, P.; Kovaříková, P.; Šimůnek, T.; Vávrová, K. Aroylhydrazone iron chelators: Tuning antioxidant and antiproliferative properties by hydrazide modifications. *Eur. J. Med. Chem.* **2016**, *120*, 97–110. [[CrossRef](#)]
36. Armstrong, C.M.; Bernhardt, P.V.; Chin, P.; Richardson, D.R. Structural Variations and Formation Constants of First-Row Transition Metal Complexes of Biologically Active Aroylhydrazones. *Eur. J. Inorg. Chem.* **2003**, *2003*, 1145–1156. [[CrossRef](#)]
37. Balachandran, K.; George, M. Oxidation with metal oxides—VI: Oxidation of benzoylhydrazones of aldehydes, ketones and 1, 2-diketones with nickel peroxide. *Tetrahedron* **1973**, *29*, 2119–2128. [[CrossRef](#)]
38. Iskander, M.; Saddeck, S. Coordination compounds of hydrazine derivatives with transition metals. XIV. Nickel (II) chelates with bidentate aroylhydrazones and their reactions with heterocyclic bases. *Inorg. Chim. Acta* **1977**, *22*, 141–147. [[CrossRef](#)]

39. Iskander, M.F.; El-Sayed, L.; Saddeck, S.; Abuo-Taleb, M.A. Coordination compounds of hydrazine derivatives with transition metals. Part 20. Nickel (II) chelates with hydroxy and methoxy-benzaldehyde arylhydrazones. An example of coordination isomerism. *Trans. Met. Chem.* **1980**, *5*, 168–172. [[CrossRef](#)]
40. Joseph, B.; Sithambaresan, M.; Kurup, M.P.; Ng, S.W. Bis { μ -N-[(E)-4-benzyloxy-2-oxidobenzylidene]-4-nitrobenzenecarbohydrazidato} bis [diaquanickel (II)] dimethylformamide tetrasolvate. *Acta Cryst.* **2014**, *70*, m211–m212. [[CrossRef](#)]
41. Ma, J.-X.; Li, Q.-L.; Li, P.-P.; Zhao, J.-X.; Zhao, L. Crystal structure of bis {5-methoxy-2-((E)-((E)-1-(methoxyimino) ethyl) phenyl) imino methyl} phenolato- κ 2N, O} nickel (II), C₃₄H₃₄N₄NiO₆. *Z. Krist.-New Cryst. Struct.* **2018**, *233*, 767–769. [[CrossRef](#)]
42. Mondal, S.; Das, C.; Ghosh, B.; Pakhira, B.; Blake, A.J.; Drew, M.G.; Chattopadhyay, S.K. Synthesis, spectroscopic studies, X-ray crystal structures, electrochemical properties and DFT calculations of three Ni (II) complexes of aryl hydrazone ligands bearing anthracene moiety. *Polyhedron* **2014**, *80*, 272–281. [[CrossRef](#)]
43. Jia, W.P.; Yang, J.G.; Li, F.; Pan, F.Y. Synthesis and Crystal Structure of a Ni (II) Complex of 2'-[4-N, N'-(Dimethylaminobenzylidene)]-3,5-dihydroxybenzoylhydrazide and Its Spectral Properties. *Chin. J. Inorg. Chem.* **2009**, 1635–1639.
44. Zhang, S.-P.; Liu, Z.-D.; Chen, S.-S.; Wei, Y.; Shao, S.-C. Synthesis, characterization and crystal structure of bis (p-fluorobenzaldehyde salicylhydrazone) nickel (II). *Chin. J. Inorg. Chem.* **2007**, *23*, 1069–1071.
45. Jia, W.P.; Yang, J.G.; Li, F.; Pan, F.Y. Synthesis and Crystal Structure of Ni (II) Complex of 2'-(4-fluorobenzylidene)]-3,5-dihydroxybenzoylhydrazide and Its Spectral Properties. *Chin. J. Inorg. Chem.* **2008**, *24*, 627–630.
46. SAINT Data Reduction Software. Version 6.45. *Bruker Analytical X-ray Systems*; Bruker AXS Inc.: Madison, WI, USA, 2003.
47. SADABS, V. 2.05; Bruker AXS Inc.: Madison, WI, USA, 2002.
48. Blessing, R.H. An empirical correction for absorption anisotropy. *Acta Cryst.* **1995**, *51*, 33–38. [[CrossRef](#)]
49. Sheldrick, G.M. A short history of SHELX. *Acta Cryst.* **2008**, *64*, 112–122. [[CrossRef](#)]
50. Barbour, L.J. *X-Seed—A Software Tool for Supramolecular Crystallography*; Elsevier: Amsterdam, The Netherlands, 2001.
51. Owuama, C.I. Determination of minimum inhibitory concentration (MIC) and minimum bactericidal concentration (MBC) using a novel dilution tube method. *Afric. J. Microb. Res.* **2017**, *11*, 977–980.
52. Arfan, M.; Khan, R.; Tavman, A.; Saba, S. Spectral characterization and crystal structure of 2-amino-N'-[(1Z)-1-(4-chlorophenyl) ethylidene]-benzohydrazide. *J. Saud. Chem. Soc.* **2016**, *20*, 40–44. [[CrossRef](#)]
53. Gluvchinsky, P.; Mockler, G.M.; Sinn, E. Nickel (II) complexes of some quadridentate Schiff-base ligands—II. Infrared spectra. *Spectro. Acta A Mol. Spect.* **1977**, *33*, 1073–1077. [[CrossRef](#)]
54. Rassem, H.; Nour, A. Synthesis, Spectral Characterization and Crystal Structure of (E)-4-Hydroxy-N-(2-Methoxybenzylidene) Benzohydrazide. *Aust. J. Bas. Appl. Sci.* **2016**, *10*, 513–516.
55. Krueve, A.; Kaupmees, K.; Liigand, J.; Oss, M.; Leito, I. Sodium adduct formation efficiency in ESI source. *J. Mass Spect.* **2013**, *48*, 695–702. [[CrossRef](#)] [[PubMed](#)]
56. Al-Odayni, A.-B.; Alfotawi, R.; Khan, R.; Saeed, W.S.; Al-Kahtani, A.; Aouak, T.; Alrahlah, A. Synthesis of chemically modified BisGMA analog with low viscosity and potential physical and biological properties for dental resin composite. *Dent. Mater.* **2019**, *35*, 1532–1544. [[CrossRef](#)] [[PubMed](#)]
57. Demarque, D.P.; Crotti, A.E.; Vessecchi, R.; Lopes, J.L.; Lopes, N.P. Fragmentation reactions using electrospray ionization mass spectrometry: An important tool for the structural elucidation and characterization of synthetic and natural products. *Nat. Prod. Rep.* **2016**, *33*, 432–455. [[CrossRef](#)] [[PubMed](#)]
58. Iskander, M.F.; El-Sayed, L.; Salem, N.M.; Werner, R.; Haase, W. Synthesis, characterization and magnetochemical studies of dicopper (II) complexes derived from bis (N-salicylidene) dicarboxylic acid dihydrazides. *J. Coord. Chem.* **2005**, *58*, 125–139. [[CrossRef](#)]
59. Arafath, M.A.; Al-Suede, F.S.; Adam, F.; Al-Juaid, S.; Khadeer Ahamed, M.B.; Majid, A.M. Schiff base-nickel, palladium, and platinum complexes derived from N-cyclohexyl hydrazine carbothioamide and 3-hydroxy-4-methoxybenzaldehyde: Selective antiproliferative and proapoptotic effects against colorectal carcinoma. *Drug. Devel. Res.* **2019**, *80*, 778–790. [[CrossRef](#)]
60. Ejidike, I.P.; Ajibade, P.A. Synthesis, characterization and biological studies of metal (II) complexes of (3E)-3-[(2-((E)-[1-(2,4-dihydroxyphenyl) ethylidene] amino) ethyl) imino]-1-phenylbutan-1-one Schiff base. *Molecules* **2015**, *20*, 9788–9802. [[CrossRef](#)]
61. Blanchard, S.; Neese, F.; Bothe, E.; Bill, E.; Weyhermüller, T.; Wiegardt, K. Square planar vs tetrahedral coordination in diamagnetic complexes of nickel (II) containing two bidentate π -radical monoanions. *Inorg. Chem.* **2005**, *44*, 3636–3656. [[CrossRef](#)]
62. Bouzerafa, B.; Ourari, A.; Aggoun, D.; Ruiz-Rosas, R.; Ouennoughi, Y.; Morallon, E. Novel nickel (II) and manganese (III) complexes with bidentate Schiff-base ligand: Synthesis, spectral, thermogravimetry, electrochemical and electrocatalytic properties. *Res. Chem. Int.* **2016**, *42*, 4839–4858. [[CrossRef](#)]
63. Angelusiu, M.V.; Barbuceanu, S.-F.; Draghici, C.; Almajan, G.L. New Cu (II), Co (II), Ni (II) complexes with aryl-hydrazone based ligand. Synthesis, spectroscopic characterization and in vitro antibacterial evaluation. *Eur. J. Med. Chem.* **2010**, *45*, 2055–2062. [[CrossRef](#)]
64. Ahmed, A.H.; Hassan, A.; Gumaa, H.A.; Mohamed, B.H.; Eraky, A.M. Nickel (II)-oxaloyldihydrazone complexes: Characterization, indirect band gap energy and antimicrobial evaluation. *Cog. Chem.* **2016**, *2*, 1–14. [[CrossRef](#)]
65. Kumar, D.; Chadda, S.; Sharma, J.; Surain, P. Syntheses, spectral characterization, and antimicrobial studies on the coordination compounds of metal ions with Schiff base containing both aliphatic and aromatic hydrazide moieties. *Bioinorg. Chem. Appl.* **2013**, 2013. [[CrossRef](#)] [[PubMed](#)]
66. Mishra, L.; Singh, V.K. Synthesis, structural and antifungal studies of Co (II), Ni (II), Cu (II) and Zn (II) complexes with new Schiff bases bearing benzimidazoles. *Indian J. Chem.* **1993**, *32*, 446–449.